EXHAUST FLOW PULSATION EFFECT ON RADIAL TURBINE PERFORMANCE

J. Fjällman - M. Mihaescu - L. Fuchs

Department of Mechanics, CCGEx, KTH Royal Institute of Technology, Stockholm 100 44, Sweden,
Email: johanf@mech.kth.se

ABSTRACT

In the current vehicle manufacturing world the chase for a better fuel economy and better driveability is in high gear. One way of doing so is to investigate and optimize the turbocharger. In this paper the flow in a radial turbine of a passenger car turbocharger has been analysed by Large Eddy Simulations. The current simulations have investigated the effects of changing the inlet pulse frequency and inlet pulse shape on turbine's performance parameters (e.g. efficiency, shaft power, pressure distributions). Three different engine speeds and two different pulse shapes were chosen to be compared and analysed. With the total mass flow per pulse being constant for all cases there is a clear dependence of both pulse shape and frequency when it comes to e.g. wheel momentum. Higher frequency increases the peak momentum more than the minimum level. A reduction in pulse duration also increases peak momentum more than the minimum.

NOMENCLATURE

ρ	Density
t	Time
x	Spatial direction
u	Velocity
i, j, k	Component x,y,z
p	Pressure
τ_{ij}	Viscous shear stress tensor
E	Total energy
q_i	Heat flux
W_{ext}	External volume forces
q_H	Added heat
R	Universal gas constant
T	Temperature
S_{ij}	Rate of strain tensor
μ	Dynamic viscosity
V	Volume
$\mathbf{v}$	Velocity magnitude

INTRODUCTION

For the vehicle industry today there is a stricter legislation from the European Union concerning emissions from road vehicles. This legislation is revised from time to time, making the acceptable levels smaller and smaller. This in turn forces the companies to create better and better engines.

One way of reducing the emission levels for an engine is to make it smaller. A smaller engine has lower losses that are tied to its geometry which makes it use less fuel. One problem with this is that with a smaller engine you also get a lower power output. To keep the same power for a smaller engine one of the more popular methods is to add a turbocharger.

The turbocharger consists of a compressor that increases the pressure of the inflow air and a turbine that drives the compressor by utilizing the available energy in the exhaust gases. A turbocharger would mean we could have a lower fuel consumption for the same power output (Silva *et al.*, 2009; Karabektas, 2009). By increasing the effectiveness of the turbine one can increase both the power output from the engine and lower the fuel consumption.

In this paper the flow associated with a radial turbocharger turbine from a passenger car has been simulated and analyzed by Large Eddy Simulations (LES). The entire exhaust manifold corresponding to a four cylinder passenger car engine is considered upstream of the turbine's geometry. At each of the four exhaust ports (inlet planes for the computational domain), pulsating inlet conditions according to three different engine speeds are considered. The inlet boundary has been simulated with two different profiles for each engine speed, giving a total of six different cases. A previous study has been performed where grid sensitivity and inlet boundary sensitivity has been assessed using LES for a non-pulsating inflow condition (Fjällman *et al.*, 2012), see also Tab. 1.

When optimizing the turbocharger to the engine there are several things to consider. The turbocharger size needs to be well matched to the engine size in order to optimize the transient response, i.e. the turbo lag. If the turbine is too large the increased wheel inertia will impair the transient response of the turbine. On the other hand if the turbine is too small it may choke during high engine speeds where the volume flow is large. The transient response is dependent not only on the turbine wheel inertia but also on the size and efficiency of the turbine. This matching has traditionally been performed using 1D-simulation tools in conjunction with compressor and turbine efficiency maps from gas-stand tests. With the current increase in computational resources this has made 3D Reynolds Averaged Navier-Stokes (RANS) models a viable option for the industry.

1D modelling tools and RANS simulations cannot account for all effects present in the flow field. There are many important and complex flow phenomena that the simpler models are unable to resolve, such as: boundary condition pulsations (e.g. Hellström & Fuchs, 2008*b*; Cao *et al.*, 2014), and flow asymmetry due to non-symmetric geometry (Marelli & Capobianco, 2011; Galindo *et al.*, 2013)). Other issues with these simpler models are that they assume that the flow is fully turbulent and regions with adverse pressure gradients might not be handled correctly. These phenomena will introduce different kinds of flow losses and structures in the flow field, which should be resolved in order to accurately predict the flow in the turbocharger. Since the turbine is sensitive to the flow upstream of the wheel the inlet manifold is simulated and it is important to resolve the flow accurately in order to predict the correct structures.

Because of these requirements the Large Eddy Simulations (LES) will be the method of choice (Dufour *et al.*, 2009). By using the LES approximation you will get the full 4D compressible flow field (3 spacial dimensions + time), this entails that the retrieved flow information is more complete and that the flow structures and losses can be studied in more depth. The LES method has been used by other researchers within the Internal Combustion Engine (ICE) area. E.g comparing experimental and numerical data related to EGR mixing homogeneity in a truck inlet manifold (Sakowitz *et al.*, 2012), comparing experimental and numerical (both LES and RANS) data for a centrifugal compressor (e.g. Guleren *et al.*, 2008; Semlitsch *et al.*, 2014; Sundström *et al.*, 2014) with the last two authors using the same solver as used in this study.

Earlier studies that have been performed for turbocharger turbines have mainly been focusing on steady inflow conditions. For example in Hellström & Fuchs (2008*a*) several inlet conditions were used in order to assess their effect on e.g. the turbine effectiveness. The results indicate that adding a secondary motion to the inlet condition changes the results much more than the kind of secondary motion used does.

METHODS

For the simulations the CFD-code Star-CCM+ v.9 by CD-Adapco has been used.

The flow governing equations for the conservation of mass, momentum, energy, and the equation of state are as follows:

$$\frac{\partial \rho}{\partial t} + \frac{\partial}{\partial x_i}(\rho u_i) = 0, \tag{1}$$

$$\frac{\partial}{\partial t}(\rho u_i) + \frac{\partial}{\partial x_j}(\rho u_i u_j) = -\frac{\partial p}{\partial x_i} + \frac{\partial \tau_{ij}}{\partial x_j}, \tag{2}$$

$$\frac{\partial}{\partial t}(\rho E) + \frac{\partial}{\partial x_i}(\rho u_i E) = -\frac{\partial}{\partial x_i}(pu_i) + \tau_{ij}\frac{\partial u_i}{\partial x_j} - \frac{\partial q_i}{\partial x_i} + W_{ext} + q_H, \tag{3}$$

$$p = \rho RT, \tag{4}$$

$$\tau_{ij} = 2\mu(S_{ij} - \frac{1}{3}S_{kk}\delta ij), \tag{5}$$

$$S_{ij} = \frac{1}{2}\left(\frac{\partial u_i}{\partial x_j} + \frac{\partial u_j}{\partial x_i}\right). \tag{6}$$

The equation of state (4) is used to close the non-linear system of equations (1) - (3).

Large Eddy Simulations were first introduced in the 60's by Joseph Smagorinsky (Smagorinsky, 1963) and quickly grew in popularity. In the 70's James Deardorff looked into some of the problems associated with LES (Deardorff, 1970). The LES method resolves the large turbulent scales and models the small scales using a Sub-Grid Scale (SGS) model. For the past 20 years an Implicit LES (ILES) method has been growing and improving (Grinstein *et al.*, 2007). The ILES method means that no explicit SGS model is being used which has its advantages and disadvantages. The method is based upon the Kolmogorov hypotheses that the small and unresolved (in LES) scales are universal and statistically isotropic. When the momentum equation is discretized a new term appears, the truncation error ϵ_t, which depends on the numerical scheme and its order. When using a second order discretization scheme the SGS model and the ϵ_t are of the same order of magnitude and because of their additive nature they are hard to separate. If the filter width is small enough you can make sure that the filtered scales are isotropic, universal, and mainly responsible for the dissipation.

The Kolmogorov hypotheses state (e.g. Pope, 2000) that the large energy containing and the small dissipative scales are separated by an area called the inertial sub-range. The inertial sub-range is independent of viscosity (ν) and depends only on the dissipation rate (ϵ). Because of this we are only interested in the amount of dissipation (i.e. numerical or modelled dissipation does not matter). Following this the need for an explicit SGS model is removed if the energy spectra is shown to contain the inertial sub-range, meaning that the spatial resolution of the grid is fine enough to support the ILES method.

One of the issues with the ILES method is that it is hard to judge if the grid resolution is fine enough a priori. One of the ways of making sure that the grid is fine enough is to analyse the Power Spectral Density (PSD) of the velocity at key locations. If a sufficient portion of the inertial sub-range is visible in the spectra the grid is deemed to be fine enough.

The ILES method has been used successfully by other researchers as well, e.g. Sakowitz *et al.* (2013) where a T-junction is investigated by the ILES method, and Garmann *et al.* (2013) who compares SGS models and the ILES method for a low Reynolds number case. In Semlitsch *et al.* (2014) and Sundström *et al.* (2014) the flow in a radial compressor is analysed, using the same solver. The

CFD results were in good comparison with both Particle Image Velocimetry (PIV) data and pressure based frequency spectras.

For the ILES computations a fully compressible density based coupled flow solver has been used. Time discretization was of second order and spatial discretization was of formal second order (bounded central differencing scheme (Leonard, 1991; Darwish & Moukalled, 1994)).

In Tab. 1 selected results from (Fjällman *et al.*, 2012) are shown, where experimental data is compared against URANS and ILES results. Here we can see large differences between the URANS and ILES results, since there are no experimental results available for the pulsating cases the mose accurate method was chosen.

Table 1: **Comparison between experimental work, URANS, and ILES. η is the efficiency, PR is the pressure ratio over the turbine and P_s is the shaft power.**

Method	η [%]	PR [-]	P_s [W]
Experiment	55.6	2.64	14 360
URANS	64.0	2.72	16 950
ILES	55.1	2.63	14 150

CASE SET-UP, BOUNDARY CONDITIONS, AND GEOMETRY

For this study three different engine speeds have been run: 1250, 1500, and 1750 RPM. Also two different inlet profiles were used, the normal profile and a Divided Exhaust Period (DEP) like profile. The DEP profile means that the exhaust valves are closing earlier (approximately 70 CAD). This leads to a lower total mass flow per pulse than for the normal profile, so the DEP profile has been scaled up to give the same mass per pulse as the normal profile. This was done in order to not have to rescale the turbine for a different average mass flow. All cases simulated with the pulsating inlet are shown in Tab. 2. These engine speeds were chosen because these are areas where you want to have a short time to torque, i.e. a fast acceleration of your car.

Table 2: **The six different cases that have been run for this study. 'A' refers to the profile and 'C' to the engine speed. See also Fig. 2 for a visualization of the profiles.**

Case	RPM	Profile
A1C1	1250	Normal
A1C2	1500	Normal
A1C3	1750	Normal
A2C1	1250	DEP
A2C2	1500	DEP
A2C3	1750	DEP

The computational domain used for this study is shown in Fig. 1.

Boundary Conditions

The inlet boundary conditions are time dependent temperature and mass flow with an added 5% turbulence intensity. The normalized profiles for the first inlet are shown in Fig. 2 for all the cases. The boundary conditions were adapted from GT-Power simulations where the mass flow and temperature were obtained just as the turbo-lag ended. The mass flows and temperatures were then compared for
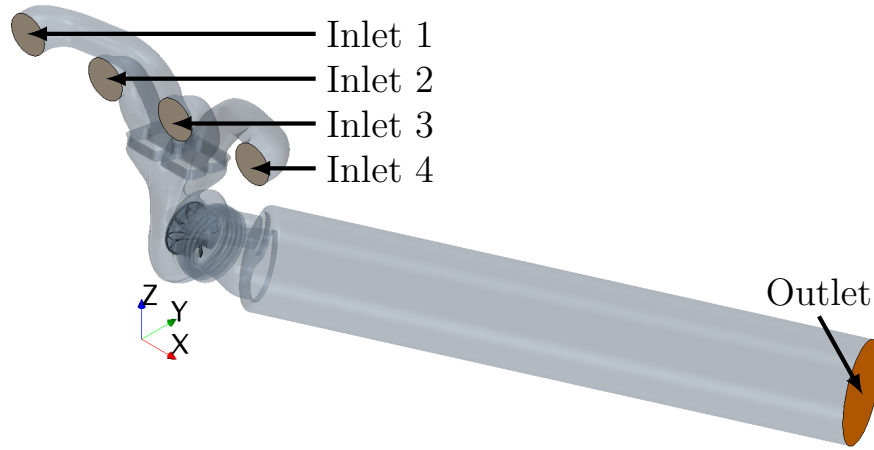
Figure 1: **Simulation geometry, inlets in grey and outlet in brown.**

the three engine speeds and since the differences were very small (<1%) the middle engine speed (1500 RPM) profile was used. The same temperature profile was used for all six cases as well.
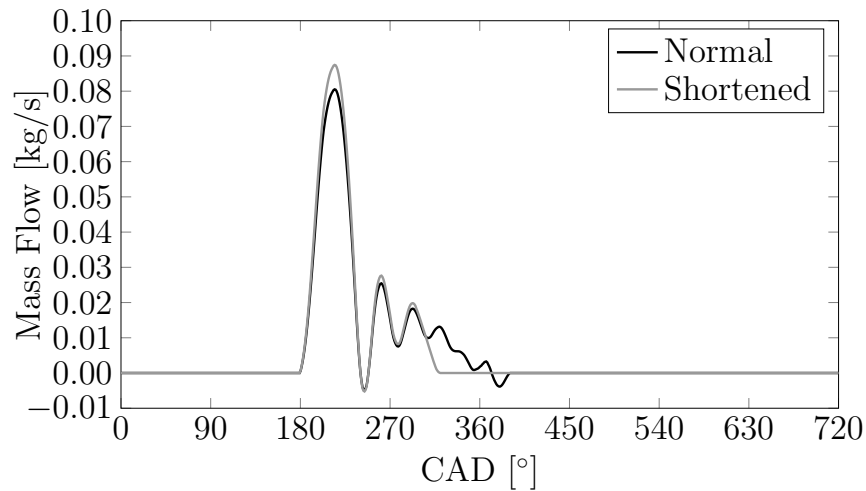

Figure 2: **Two different inlet profiles that have been used. The normal one in black and the shortened profile in grey.**

The shortened profile was created by artificially closing the valve 70 CAD earlier. The total injected mass was then calculated for the normal profile and the shortened profile was scaled to match the same total injected mass per pulse.

The outlet after the turbine was extruded another 500 mm to damp the outlet reflections and a constant pressure was set. The chosen pressure was the mean of the turbine exit pressure from the GT-Power simulations. The walls were set to adiabatic and no-slip. The wheel rotation was handled by the sliding mesh technique, where the grid is made to physically rotate around the turbine wheel axis. This is a more physical approach than using a rotating reference frame.

Grids

The grid used for this study is adapted from the grid used in Fjällman *et al.* (2014) with the outer shell removed. This was performed in order to speed up the simulation convergence time. The grid

consists of ≈4 million cells in total. With ≈1.5 million cells in the turbine wheel and ≈2.5 million cells in the rest of the geometry, with a higher cell density in the volute and areas around the turbine wheel, see Fig. 3.
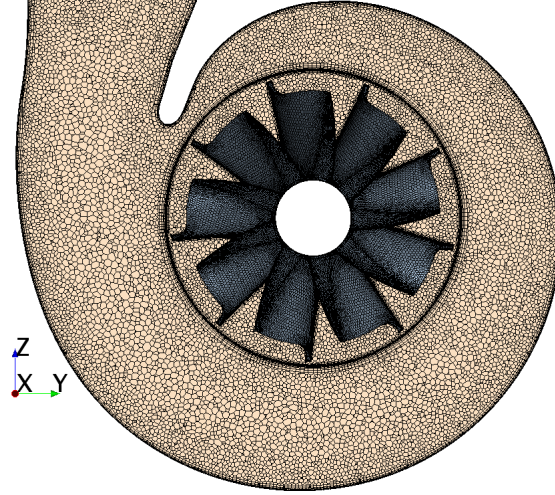

Figure 3: **The grid used for all simulations. The mesh density is increased close to the wheel and on the wheel tips, for a smoother edge.**

The grid uses five prism layers along the walls in the volute and wheel areas, with a reduction to two prism layers in the outlet and inlet pipe regions.

A grid sensitivity study was performed in an earlier study, see Fjällman *et al.* (2012).

RESULTS

In order to evaluate the results one can look at the wheel torque being generated by the flow or the kinetic energy available. In Fig. 4 the wheel torque is shown for the 1250 RPM case. The shortened profile case (A2) is seen to have a constantly higher wheel torque, even when there is no flow entering the domain.

The wheel torque for the other cases are shown in Figs. 5 and 6. It can be seen that the differences between the profiles are decreasing with increasing RPM. One can also see that the outer cylinders, 1 and 4, have a higher peak torque.

By integrating the wheel torque for each pulse one can estimate and compare the different pulses more easily. In Fig. 7 the integrated values are shown, the outer cylinders are shown to have a larger integrated torque as well. This difference is ≈1-2%, which is small and most likely not significant, but still present.

By integrating the kinetic energy from the inlets and comparing it to the kinetic energy entering and leaving the turbine wheel region one can get an estimate of the energy efficiency of the system. In Tab. 3 the kinetic energy efficiency is shown according to Eq. 7.

$$\eta_{KE} = \frac{\int \frac{\rho V_1 \mathbf{v}_1^2}{2}}{\int \frac{\rho V_2 \mathbf{v}_2^2}{2} - \int \frac{\rho V_3 \mathbf{v}_3^2}{2}}. \tag{7}$$

In Eq. (7), position 1 is at the inlet of the geometry, position 2 is before the turbine wheel and position 3 is after the turbine wheel.

By studying Tab. 3 one can see that the outer cylinders (1 and 4) consistently have a higher efficiency than the inner cylinders. One can also see that the shortened profile has a higher efficiency
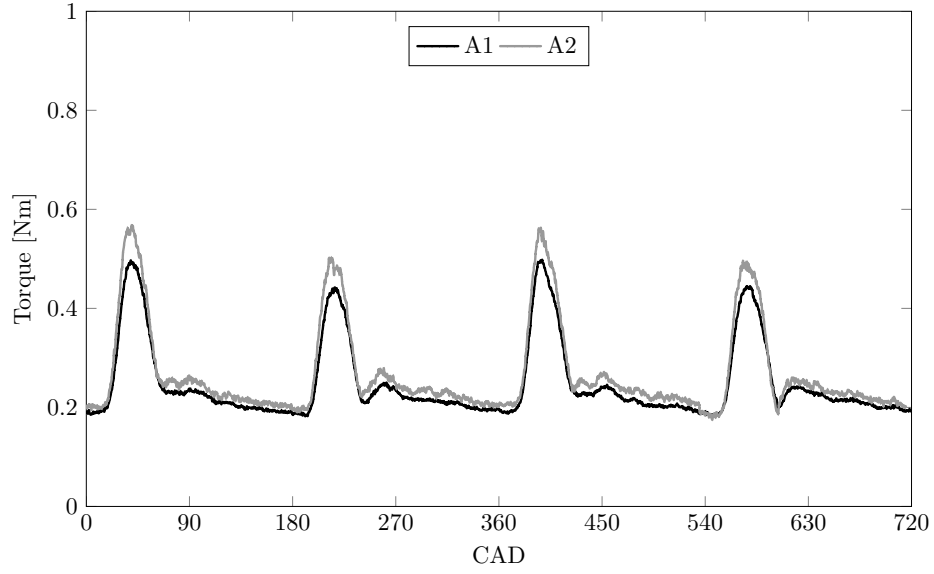
Figure 4: **The wheel torque is shown for both profiles for the first case (1250 RPM). The peaks correspond to cylinders 1, 3, 4, and 2.**
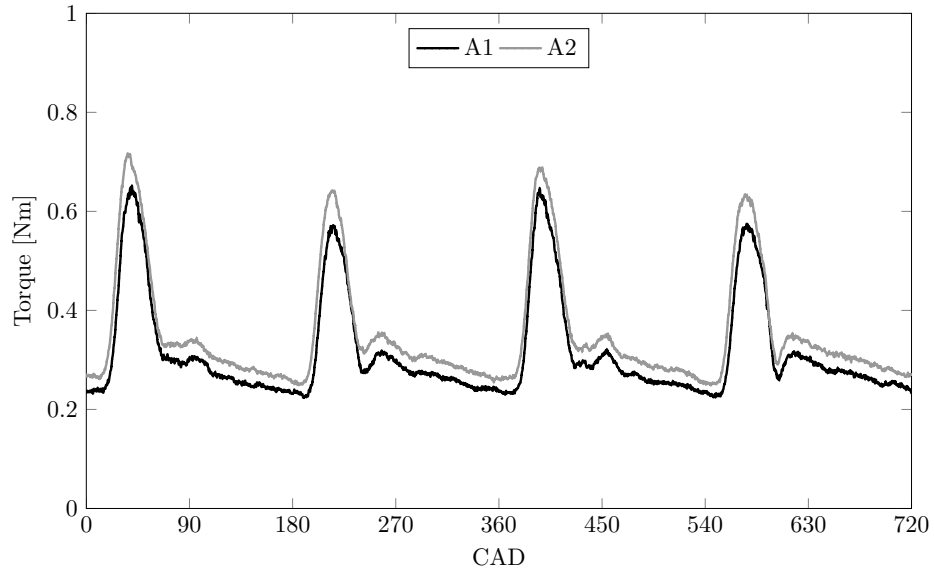

Figure 5: **The wheel torque is shown for both profiles for the second case (1500 RPM). The peaks correspond to cylinders 1, 3, 4, and 2.**

than the normal profile, except for the 1500 RPM case (C2) where the efficiency is the same. The efficiency increase is also reduced as the engine speed reduces.

CONCLUSIONS

In this paper we have shown that the pulse shape and frequency is affecting the torque and integrated torque in several ways. The shortened profile has a higher peak mass flow which will increase the blow down pulse peak. In the results one can see that the peak torque is increased by $\approx 12\%$ but also that the minimum torque levels are higher for the shortened profile. This behaviour was not
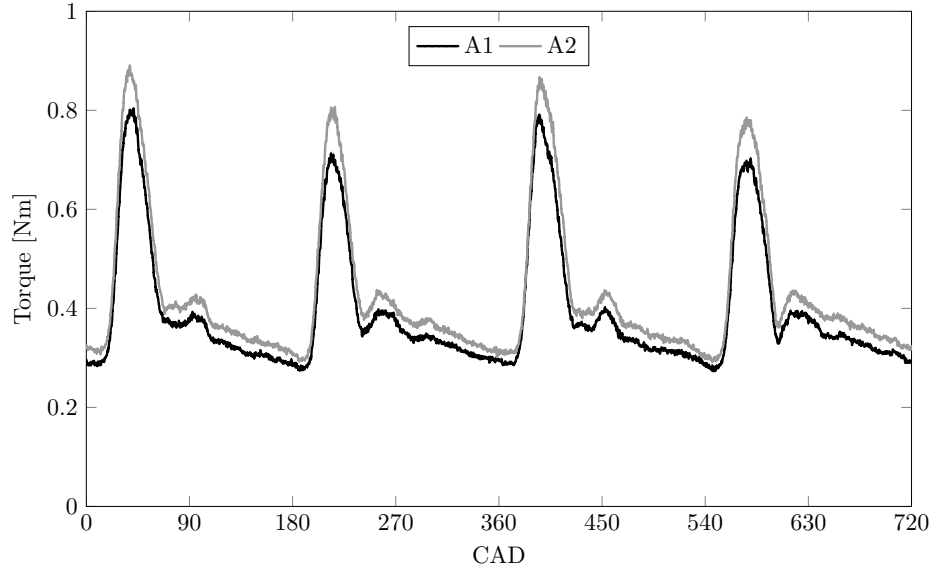
Figure 6: **The wheel torque is shown for both profiles for the third case (1750 RPM). The peaks correspond to cylinders 1, 3, 4, and 2.**
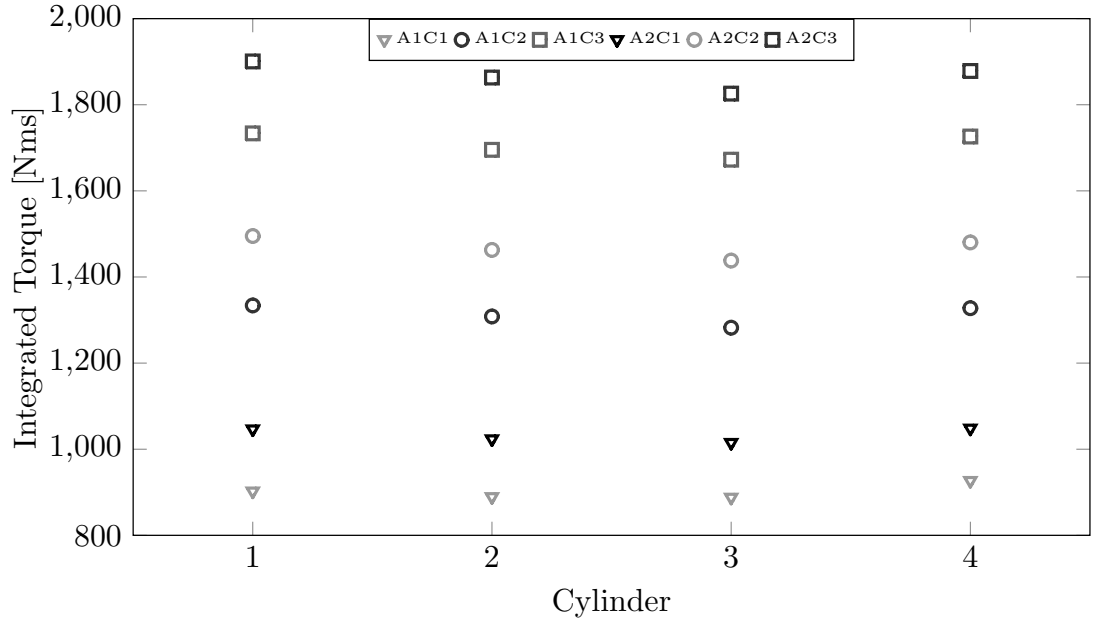

Figure 7: **The integrated wheel torque is shown for all cases and profiles. The differences between normal and short profile is reduced as the engine speed is increased. A1 is normal profile, A2 is shortened profile. C1 is 1250 RPM, C2 is 1500 RPM, and C3 is 1750 RPM.**

expected since the flow into the geometry stops 70 CAD earlier in the shortened profile case. This phenomena is hypothesized to partly be an effect of the geometry volume. The volute and exhaust manifold volume will act as a damper for the system, storing parts of the flow energy to be used later.

The differences seen between the cylinders are very small ($\approx$1-2%) and most likely not significant for the power production. Although, this might be an indication of how to optimize the geometry. If one can optimize the bends and in flow angles into the volute the power from the turbine should

Table 3: **The kinetic energy efficiency for the different cases and cylinders.**

Case	Cylinder 1	Cylinder 2	Cylinder 3	Cylinder 4
A1C1	59%	55%	54%	57%
A1C2	65%	59%	58%	64%
A1C3	61%	56%	56%	60%
A2C1	71%	63%	62%	69%
A2C2	65%	60%	58%	64%
A2C3	65%	60%	60%	65%

be able to be increased. It should also be possible to perform these changes within the same outer volumes, keeping the engine packaging constraints intact.

The kinetic energy efficiency shows us that the outer cylinders have a higher efficiency than the inner cylinders. It is also seen that the 1500 RPM case shows little to no increase in efficiency, whereas the two other cases shows 5-10% increase in efficiency. With the shorter profile being the one with the higher efficiency.

References

CAO, T., XU, L., YANG, M. & MARTINEZ-BOTAS, R. F. 2014 Radial turbine rotor response to pulsating inlet flows. *Journal of Turbomachinery* **136** (7), 071003.

DARWISH, M. & MOUKALLED, F. 1994 Normalized variable and space formulation methodology for high-resolution schemes. *Numerical Heat Transfer* **26** (1), 79–96.

DEARDORFF, J. W. 1970 A numerical study of three-dimensional turbulent channel flow at large Reynolds numbers. *Journal of Fluid Mechanics* **41** (02), 453–480.

DUFOUR, G., GOURDAIN, N., DUCHAINE, F., VERMOREL, O., GICQUEL, L., BOUSSUGE, J. & POINSOT, T. 2009 Large eddy simulation applications. *VKI Lecture Series* .

FJÄLLMAN, J., MIHAESCU, M. & FUCHS, L. 2012 Effects of inlet geometry on turbine performance. In *Proceedings of International Conference on LES for Internal Combustion Engine Flows, LES4ICE*.

FJÄLLMAN, J., MIHAESCU, M. & L., F. 2014 Analysis of 3 dimensional turbine flow by using mode decomposition techniques. In *ASME Turbo Expo*. ASME.

GALINDO, J., FAJARDO, P., NAVARRO, R. & GARCÍA-CUEVAS, L. 2013 Characterization of a radial turbocharger turbine in pulsating flow by means of CFD and its application to engine modeling. *Applied Energy* **103**, 116–127.

GARMANN, D. J., VISBAL, M. R. & ORKWIS, P. D. 2013 Comparative study of implicit and subgrid-scale model large-eddy simulation techniques for low-Reynolds number airfoil applications. *International Journal for Numerical Methods in Fluids* **71** (12), 1546–1565.

GRINSTEIN, F. F., MARGOLIN, L. G. & RIDER, W. J. 2007 *Implicit large eddy simulation: computing turbulent fluid dynamics*. Cambridge University Press.

GULEREN, K., TURAN, A. & PINARBASI, A. 2008 Large-eddy simulation of the flow in a low-speed centrifugal compressor. *International journal for numerical methods in fluids* **56** (8), 1271–1280.

HELLSTRÖM, F. & FUCHS, L. 2008*a* Effects of inlet conditions on the turbine performance of a radial turbine. In *ASME Turbo Expo 2008: Power for Land, Sea, and Air*, pp. 1985–2001. American Society of Mechanical Engineers.

HELLSTRÖM, F. & FUCHS, L. 2008*b* Numerical computations of pulsatile flow in a turbo-charger. In *AIAA-46th Aerospace Sciences Meeting*.

KARABEKTAS, M. 2009 The effects of turbocharger on the performance and exhaust emissions of a diesel engine fuelled with biodiesel. *Renewable Energy* **34** (4), 989–993.

LEONARD, B. 1991 The ultimate conservative difference scheme applied to unsteady one-dimensional advection. *Computer methods in applied mechanics and engineering* **88** (1), 17–74.

MARELLI, S. & CAPOBIANCO, M. 2011 Steady and pulsating flow efficiency of a waste-gated turbocharger radial flow turbine for automotive application. *Energy* **36** (1), 459–465.

POPE, S. 2000 *Turbulent flows*. Cambridge University Press.

SAKOWITZ, A., MIHAESCU, M. & FUCHS, L. 2013 Effects of velocity ratio and inflow pulsations on the flow in a T-junction by large eddy simulation. *Computers & Fluids* **88**, 374–385.

SAKOWITZ, A., REIFARTH, S., MIHAESCU, M. & FUCHS, L. 2012 Modeling of EGR mixing in an engine intake manifold using LES .

SEMLITSCH, B., JYOTHISHKUMAR, V., MIHAESCU, M., FUCHS, L., GUTMARK, E. & GANCEDO, M. 2014 Numerical flow analysis of a centrifugal compressor with ported and without ported shroud. *Tech. Rep.* 2014-01-1655. SAE Technical Paper.

SILVA, C., ROSS, M. & FARIAS, T. 2009 Analysis and simulation of "low-cost" strategies to reduce fuel consumption and emissions in conventional gasoline light-duty vehicles. *Energy Conversion and Management* **50** (2), 215–222.

SMAGORINSKY, J. 1963 General circulation experiments with the primitive equations: I. the basic experiment. *Monthly weather review* **91** (3), 99–164.

SUNDSTRÖM, E., SEMLITSCH, B. & MIHAESCU, M. 2014 Assessment of the 3D flow in a centrifugal compressor using steady-state and unsteady flow solvers. *Tech. Rep.* 2014-01-2856. SAE Technical Paper.